Oscillating Laminar Boundary Layers and Unsteady Separation

D. TH. TSAHALIS* AND D. P. TELIONIS†
Virginia Polytechnic Institute and State University, Blacksburg, Va.

The unsteady laminar boundary-layer equations are solved numerically for oscillating outer flow velocity distributions. Some characteristic features of oscillating boundary layers are observed and checked against existing analytical and experimental data. The response of the point of zero skin friction that marks flow reversal on the wall, to various outer flow oscillatory distributions is investigated. The phenomenon of steady streaming is studied numerically for external flows with a nonvanishing mean. The point of unsteady separation as defined by Sears and Telionis and Despard and Miller is found to be shifted upstream of the location of steady state separation that corresponds to the mean outer flow velocity distribution.

I. Introduction

UNSTEADY aerodynamic phenomena may often be effectively represented by quasi-steady models. In many modern applications though such as missiles and in general unmanned vehicles, high accelerations invalidate the assumption of quasi-steady flow. Problems of the flutter category, for example, rotating stall in axial flow compressors and stalling flutter of an airfoil, also involve nonnegligible unsteady viscous flow effects. Lighthill[1] studied for the first time in 1954 the response of a laminar boundary layer to small oscillations of the outer flowfield, $U(s,t) = U_0(s) + \varepsilon U_1(s)e^{i\omega t}$, where U is the outer flow velocity, and s and t are the distance along the wall and time, respectively. He indicated that for small ε and for large frequencies and/or distances from the leading edge, the solution tends to a Stokes shear wave and for small frequencies and/or distances from the leading edge, he proposed a solution based on the Kármán-Polhausen method. Rott[2] and Glauert[3] have independently considered stagnation flow on an oscillating plane. Rott and Rosenzweig[4] and Lam and Rott[5] extended the work of Lighthill and later Ackerberg and Phillips[6] reconsidered the problem and formalized the procedure in order to join rigorously the asymptotic expansions valid in different domains of the flowfield. Lin[7] and Gibson[8] considered the same problem with larger values of ε but $\varepsilon < 1$.

The range of validity of the above solutions is confined by assumptions like extreme values of frequency, small values of ε and $U_0(s) = U_1(s)$. Such limitations can be waived only by employing numerical methods to solve the unsteady boundary-layer equations. Hall[9] developed a scheme of numerical integration but considered only an impulsive change of the outer flow. Phillips and Ackerberg[10] proposed an improved numerical scheme of integration with variable mesh size across the boundary layer and considered oscillating outer flows with no pressure gradients. Telionis, Tsahalis, and Werle[11] reported on the effect of pressure gradients but considered only transient or impulsive changes of the outer flow. The present paper reports on the results of a numerical investigation of an oscillating boundary layer with adverse pressure gradients.

There have been rather limited efforts to investigate this problem experimentally.[12,13] Moreover, both analytical and experimental methods seem to experience considerable difficulties in regions of strong adverse pressure gradients and especially as separation is approached. The most recent experimental effort to examine the region of separation and meaningfully interpret the experimental results is due to Despard and Miller.[14] By the term separation we mean here the station along the wall where the fluid breaks away from the solid boundary into the mean flow, a separated bubble or a wake is initiated and the boundary-layer approximation breaks down. For a detailed account of the terminology often found in literature and various concepts related to the phenomenon of separation the reader is referred to the review paper of Sears and Telionis.[15] The reader is only cautioned here to the fact that for unsteady flow, Prandtl's classical criterion of vanishing skin friction fails to predict separation.[15-17] Despard and Miller found experimentally that for the frequency range they examined, the location of separation is rather insensitive to the oscillations of the outer flow. They then observed that all the characteristic features of separation appear at the station of "the initial occurrence of zero velocity or reverse flow at some point in the velocity profile, throughout the entire cycle of oscillation" and they defined this station as "laminar boundary-layer separation in oscillating flows." Schneck and Ostrach[18] have later successfully used this definition to study internal flows with immediate applications to the blood flow in arterial vessels.

In general, one would expect that the point of separation would respond, with some phase angle, to the oscillations of the outer flow. Evidently, as the frequency $\omega \to 0$, the flowfield tends to become quasi-steady and the point of zero skin friction, which then coincides with the point of separation would oscillate so that instantaneously it would be located at the point of separation of the corresponding steady-state flow. The experiments of Despard and Miller therefore indicate that as the frequency increases the amplitude of oscillation of the point of separation quickly decreases due to the unsteady effects. Separation then appears to be stationary but displaced upstream from the location that corresponds to steady separation with outer flow the mean of the oscillating outer flow.

Sears and Telionis[17] based their definition of transient separation on the appearance of the separation singularity which was extensively studied in literature.[19] They defined as unsteady separation, the streamwise station where the familiar properties of a separation singularity and not necessarily a vanishing wall

Presented as Paper 74-100 at the AIAA 12th Aerospace Sciences Meeting, Washington, D.C., January 30–February 1, 1974; submitted February 20, 1974; revision received May 10, 1974. This research was supported by the Air Force Office of Scientific Research and monitored under the technical supervision of P. Thurston under Grant AFOSR-72-2361A. The authors are thankful to D. J. Schneck for some stimulating discussions. The U.S. Government is authorized to reproduce and distribute reprints for governmental purposes notwithstanding any copyright notation hereon.

Index categories: Boundary Layers and Convective Heat Transfer—Laminar; Nonsteady Aerodynamics.

* Research Associate, Engineering Science and Mechanics Department; now with Shell Oil Co., Houston, Texas. Member AIAA.

† Assistant Professor of Engineering Science and Mechanics. Associate Member AIAA.

shear, appear. In later publications[11,20,21] this definition was used to study the response of separation to transient outer flows that impose a monotonic steepening of the adverse pressure gradient as time increases. It is the purpose of the present paper to test qualitatively the definition of Sears and Telionis against the results of Despard and Miller.

The unsteady boundary-layer equations for two-dimensional flow are a set of differential equations parabolic in time t and the coordinate s along the wall. This integration should proceed in the positive direction of t and s provided that the dependent variable u, the s-component of velocity, is positive. As a result of this fact, the applicability of the mathematical model is constrained as follows. First, integration in regions of reversed flow, that is negative u, has to proceed in the opposite s-direction. This difficulty was overcome numerically by an appropriate differencing scheme as described in previous publications.[11,20] Second, the domain of integration in the s direction may not expand. If, for example, it is attempted to proceed integrating in the s-direction, beyond the final station (s_0, t_0), then information would be needed at the station $s_0+\Delta s$ of the previous time plane, $t_0-\Delta t$, which is not available. Phillips and Ackerberg[10] have achieved expansion of their domain of integration by virtue of an exact solution valid for $s > s_0$. The problem becomes more difficult if in the neighborhood of s_0 the velocity profile is partially reversed. In this case, the domain of integration should be ever collapsing as described in Refs. 11, 15, 20, and 21. This implies that a boundary-layer calculation could never solve the problem of a downstream moving separation, since the station of separation is a natural upper limit of the domain of integration. Consequently, the case of an oscillating point of separation is also forbidden, but we undertook here a calculation of oscillating boundary layers only because Despard and Miller indicated that for reasonably high frequencies, the point of separation remains unaffected during a period of oscillation. Since portions of the flow are reversed though, it is not possible mathematically to derive a solution steady in the mean, in the neighborhood of separation. We choose here an outer flow distribution that is steady in the mean but we start the calculations in such a way that the boundary layer goes through a transitional time interval corresponding to an upstream moving point of separation. Various properties of the flowfield are compared against numerical and experimental solutions. The neighborhood of separation is studied for the first time analytically and features like time lag or advance of various flow properties are investigated. The phenomenon of steady streaming has been studied up to now only analytically and mostly for cases of purely oscillatory flow.[22,23] Perhaps the use of this term may not be justified for nonvanishing outer mean flows but we propose to retain it. We therefore "define here as streaming phenomena any departure of the mean of properties from their steady value derived with outer flow distribution the mean of the outer flow oscillation." In the present paper the phenomenon is studied numerically for an oscillating outer flow with a nonvanishing mean.

II. Governing Equations

The numerical scheme of calculation of the unsteady boundary-layer equations employed by the authors up to the present[11,20,21] was based on a modified Görtler transformation. This transformation appeared to be convenient for calculations of transient flows, even though the mesh configuration of the physical plane (s, N) was not rectangular. For oscillatory flows it was found necessary to introduce a new transformation that leaves both the (s, N) and (ξ, η) mesh configurations rectangular.

Consider the general form of the unsteady boundary-layer equations

$$\partial u^*/\partial s^* + \partial v^*/\partial n^* = 0 \tag{1}$$

$$\frac{\partial u^*}{\partial t^*} + u^*\frac{\partial u^*}{\partial s^*} + v^*\frac{\partial u^*}{\partial n^*} - \frac{\partial U_e^*}{\partial t} - U_e^*\frac{\partial U_e^*}{\partial s^*} = \nu\frac{\partial^2 u^*}{\partial n^{*2}} \tag{2}$$

where s^* and n^* are the distances and u^* and v^* the velocity components parallel and perpendicular to the solid boundary, respectively, U_e^* is the outer flow velocity, and ν is the kinematic viscosity. Let U_R^* and L^* be a typical velocity and length, respectively, of the problem under consideration. Dimensionless velocities, distances, and time are then introduced according to

$$u = u^*/U_R^*, \quad v = v^* R_R^{1/2}/U_R^*, \quad U_e = U_e^*/U_R^* \tag{3}$$

$$s = s^*/L^*, \quad N = n^* R_R^{1/2}/L^* \tag{4}$$

$$t = t^* U_R^*/L^* \tag{5}$$

where R_R is a Reynolds number based on the velocity U_R^*; $R_R = U_R^* L^* \nu^{-1}$.

Equations (1) and (2) then become

$$\partial u/\partial s + \partial v/\partial N = 0 \tag{6}$$

$$\frac{\partial u}{\partial t} + u\frac{\partial u}{\partial s} + v\frac{\partial u}{\partial N} - \frac{\partial U_e}{\partial t} - U_e\frac{\partial U_e}{\partial s} = \frac{\partial^2 u}{\partial N^2} \tag{7}$$

Let us now introduce a modified Görtler transformation in the form

$$\xi = \int_0^s U_{em}\,ds \tag{8}$$

$$\eta = U_{em}(2\xi)^{-1/2} N \tag{9}$$

$$\tau = t \tag{10}$$

where $U_{em}(s)$ is an arbitrary outer velocity distribution, independent of time. It was found convenient to choose for $U_{em}(s)$, the mean $U_0(s)$ of the outer flow distribution. Note that this transformation, unlike the one introduced in previous publications, is independent of time. The transformed velocity components F and V are defined in a slightly different manner than before

$$F = u/U_e \tag{11}$$

$$V = \frac{(2\xi)^{1/2}}{U_{em}} v + \frac{2\xi U_e}{U_{em}^2}\frac{\partial \eta}{\partial s} F \tag{12}$$

so that F tends to 1 at the edge of the boundary layer and the continuity equation (6) reads

$$B_1(\partial F/\partial \xi) + B_2 F + \partial V/\partial \eta = 0 \tag{13}$$

where

$$B_1 = 2\xi U_e/U_{em} \tag{14}$$

$$B_2 = \frac{2\xi}{U_{em}^2}\left(\frac{\partial U_e}{\partial s} - \frac{U_e}{U_{em}}\frac{\partial U_{em}}{\partial s} + \frac{U_e U_{em}}{2\xi}\right) \tag{15}$$

Notice that for $U_e = U_{em}$, B_1, and B_2 reduce to 2ξ and 1, respectively, and the transformation reduces to that of Ref. 11.

Let β and β_m be the pressure gradient parameters dependent and independent of time, respectively, and defined by

$$\beta = \frac{2\xi}{U_e}\frac{dU_e}{d\xi}, \quad \beta_m = \frac{2\xi}{U_{em}}\frac{\partial U_{em}}{\partial \xi} \tag{16}$$

Then, the momentum equation (7) becomes

$$\frac{\partial^2 F}{\partial \eta^2} + A_1^*\frac{\partial F}{\partial \eta} + A_2^* F + A_3^* + A_4^*\frac{\partial F}{\partial \xi} + A_5^*\frac{\partial F}{\partial \tau} = 0 \tag{17}$$

where

$$A_1^* = -V \tag{18}$$

$$A_2^* = -\frac{2\xi}{U_{em}^2 U_e}\frac{\partial U_e}{\partial \tau} - \beta\frac{U_e}{U_{em}} F \tag{19}$$

$$A_3^* = \frac{2\xi}{U_{em}^2 U_e}\frac{U_e}{\partial \tau} + \beta\frac{U_e}{U_{em}} \tag{20}$$

$$A_4^* = -2\xi(U_e/U_{em})F \tag{21}$$

$$A_5^* = -2\xi/U_{em}^2 \tag{22}$$

The abovementioned equation is again brought in the form of a steady-state equation by introducing a difference form of the time derivative in terms of the value of F at $\tau-\Delta\tau$, which we denote here by F^0

$$\frac{\partial^2 F}{\partial \eta^2} + A_1\frac{\partial F}{\partial \eta} + A_2 F + A_3 + A_4\frac{\partial F}{\partial \xi} = 0 \tag{23}$$

where now

$$A_1 = A_1^*, \quad A_2 = A_2^* + A_5^*/\Delta\tau \tag{24}$$

$$A_3 = A_3^* - A_5 F^0/\Delta\tau, \quad A_4 = A_4^* \tag{25}$$

Equation (23), with coefficients given by Eqs. (24) and (25), is a nonlinear differential equation which together with Eq. (13) can be solved numerically by the subroutine developed by Blottner, Davis et al.[24]

III. Oscillatory Outer Flows

Calculations were performed for unsteady flows that oscillate harmonically about a Howarth outer flow distribution, that is a linearly retarded flow of the form

$$U_0^*(s^*) = U_\infty^* - b_1^* s^* \tag{26}$$

where U_∞^* is the freestream mean velocity and b^* is a constant.

If only the magnitude of the oncoming stream oscillates about a mean, then the velocity distribution on the boundary of a solid body has the form

$$U_e^*(s^*) = U_0^*(s^*) + U_1^*(s^*)\cos(\omega^* t^*) \tag{27}$$

where $U_1^*(s^*) = CU_0^*(s^*)$[1] and where C is a constant.[1] C is often assumed to be small when analytical methods are employed but this restriction does not carry over to numerical methods. In this study we took the typical length L^* to be a fixed portion of the distance to steady separation as suggested by Hill[12] in order to facilitate comparison of our results with this reference. The reference velocity, following again Hill, was assumed to be $U_R^* = U_\infty^* - b_1^* L^*$. With the dimensionless variables

$$b_1 = b_1^* L^*/U_\infty^*, \quad \omega = L^*\omega^*/U_R^* \tag{28}$$

Lighthill's oscillatory flow, with a Howarth mean distribution, takes the form

$$U_e = \frac{U_\infty^*}{U_R^*}(1 - b_1 s) + C\frac{U_\infty^*}{U_R^*}(1 - b_1 s)\cos\omega t \tag{29}$$

and by virtue of the definition of U_R^*,

$$U_e = (1 - b_1 s)(1 - b_1)^{-1}(1 + C\cos\omega t) \tag{30}$$

For Howarth's distribution we calculated that the distance to separation is given by $s = 1.222$. Note that Lighthill's oscillation in this case leaves the quasi-steady location of separation, that is the point of zero skin friction unaffected. In other words, all steady-state solutions corresponding to instantaneous outer flow distributions give a zero skin friction at a fixed point on the wall, the point $s = 1.222$.

A second outer flow distribution employed is a constant amplitude oscillation about a Howarth distribution. That is the one given by Eq. (27) with $U_1^* = \text{const}$ and U_0^* given by Eq. (26). In nondimensional form

$$U_e = (1 - b_1 s)/(1 - b_1) + U_1\cos\omega t \tag{31}$$

The above mentioned distribution resembles mostly the oscillations of the mean flow achieved experimentally by Despard and Miller,[14] at least in the neighborhood of the point of separation. Although not explicitly stated, except in his analytical derivation, this seems to be also the distribution of Hill.[12] Yet it appears that the oscillations represented by Eqs. (30) and (31) do not give rise to considerable differences in the features of separating flow.

A third distribution tried is given in its nondimensional form by

$$U_e = (1 - b_1 s)/(1 - b_1) + \cdots + Cb_1 s(1 - b_1)^{-1}\cos\omega t \tag{32}$$

This distribution leaves the outer flow independent of oscillations at $s = 0$. It should be noted that our numerical scheme of calculations was actually designed to converge to a stagnation profile at the point $s = 0$, thus solving again the classical Hiemenz problem. In the present analysis though the outer velocity U_e is not zero at $s = 0$. Hence our origin, $s = 0$, is neither a stagnation point nor a leading edge, but can be thought of as an initial station for our calculations where the boundary layer has already developed a velocity profile. We emphasize, though, that the downstream features of the flow appear to be very little affected and we were able to verify Howarth's main results and the features of separation for steady flow. With this in mind, we can now envision the distribution given by Eq. (32) as representing some change in the configuration of the solid body like the extension of a flap or even the change of the angle of attack.

In the sequel, we will refer to the distributions represented by Eqs. (30–32) by the Roman numerals I–III, respectively.

IV. Method of Solution

The system of the nonlinear parabolic equations (13) and (23) is solved implicitly by a subroutine developed by Werle and Davis.[24] At first, the steady-state equation is solved for one of the outer flow distributions as explained below in order to generate the initial flowfield. All the information in the (ξ, η) plane for $t = 0$ is stored, time is incremented, and the integration is repeated starting from $\xi = 0$, while the new data replace the old in the storage. For the outer flow distribution given by Eq. (30) (flow I), the initial flowfield is calculated with the steady-state outer flow, $U_e = (1 - b_1 s)(1 + C)(1 - b_1)^{-1}$; that is, the one that corresponds to $t = 0$. For the outer flow represented by Eq. (31) (flow II) the initial flowfield is calculated by $U_e = (1 - b_1 s)/(1 - b_1) + U_1$ and for the flow represented by Eq. (32) (flow III) the initial flowfield is calculated by $U_e = (1 - b_1 s)/(1 - b_1) + Cb_1 s/(1 - b_1)$. Note that at $t = 0$ the time derivative of all outer velocity distributions is zero.

In regions where the u-velocity component changes sign, nonlinearity reverses the proper direction of integration. This requires a proper differencing scheme, an upwind differencing scheme or a zigzag scheme which the authors have used in various combinations in previous publications.[20,21] In the present paper the following form of the ξ-derivative was used in regions of reversed flow

$$\left.\frac{\partial F}{\partial \xi}\right|_k = \frac{1}{2\Delta\xi}[(F_{k+1}^0 - F_k^0) + (F_k - F_{k-1})] \tag{38}$$

The mesh size was variable in the η-direction with a fine mesh next to the wall, in order to accurately describe the larger gradients in the vicinity of the wall as described in Sec. V. $\Delta\eta$ was taken to be 0.004 at the wall and was increased successively by a factor of 1.08 at each mesh point. There were 81 mesh points in the vertical direction and 256 stations in the ξ-direction with $\Delta\xi = 0.005$, representing altogether 20736 mesh points in the (ξ, η) plane.

As mentioned in the introduction, if at the plane $t_0 - \Delta t$ there exists reversed flow at the final station, s_0, then to allow sweeping of the t_0-plane all the way to s_0 one needs information from downstream of s_0. In our case the station s_0 coincides with separation and hence no information is available at any $s > s_0$. It is therefore imperative to quit the downstream marching in the plane t_0 at a station $s_t < s_0$. The station s_t should be determined by two conditions. The first requires that at least one mesh point is abandoned at each time plane. The second requires that any messages from downstream traveling in the negative s-direction with the maximum of the reversed flow velocity, $u_{\max}$, have not arrived at s_t in the time interval $\Delta\tau$. Let u_p be equal to $\Delta s/\Delta t$ and u_d equal to $u_{\max}$, respectively. The functions

$$s_1(t) = \int_0^t u_p\,dt \quad \text{and} \quad s_2(t) = \int_0^t u_d\,dt$$

then define two paths in the (s, t) plane that describe the collapsing of the domain of integration in the s-direction; that is at each time t_0, the integration should terminate at a station $s_t(t_0)$, such that

$$s_t(0) - s_t(t_0) > \max[s_1(t_0), s_2(t_0)]$$

V. Oscillating Boundary Layers—Streaming

The main properties of oscillating boundary layers were described by Lighthill.[1] Stuart[23] later reviewed the features of oscillatory flows with a zero mean. The previously mentioned

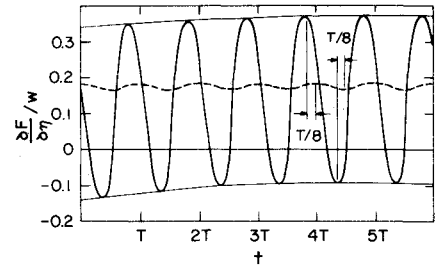

Fig. 1 Wall shear at $s \cong 0.999$ for $\omega = 3.16$, $b_1 = 0.1$, $C = 0.1$, and flow I; ------, quasi-steady; ————, unsteady.

references and the ones mentioned in the introduction can be grouped into two categories. Papers that deal with oscillating flows with nonvanishing mean that do not mention at all the phenomenon of steady streaming with the exception of Ref. 7 and papers that study the above phenomenon but consider oscillatory flows with a vanishing mean. Of course in some of the papers of the first category, zero mean pressure gradient was assumed, which precludes the appearance of steady streaming.

For oscillating flows with or without mean there exists a thin layer immediately next to the wall, where the unsteady terms are balanced by the viscous terms in the momentum equation. This layer is known in literature by the term "shear wave,"[1] "inner layer,"[2,3] "Stokes shear wave,"[6] and has a thickness δ_{in} of the order of $(\nu/\omega)^{1/2}$. Based on the Reynolds number of the streaming phenomenon, $R_s = (U_R^*)^2(\omega^*\nu)^{-1}$, we can also define the thickness δ_s of the layer where the steady streaming phenomenon is important; $\delta_s = L^*(\omega^*\nu)^{1/2}(U_R^*)^{-1}$. Note that the ratio, δ_{in}/δ_s is equal to Stuart's parameter $\alpha = U_R^*/\omega^* L^*$.

Some typical results are depicted in Fig. 1 where for the flow distribution I, we have calculated the wall shear for the quasi-steady and the purely unsteady case. The wall is the lower limit of the Stokes layer and therefore a 45° phase advance is expected and found numerically between the two functions as marked in the figure in terms of the period. Note also that the unsteady variation is much more pronounced and that the phenomenon of streaming is evident since the mean of the quasi-steady variation is considerably larger than the mean of the unsteady variation. For the flow distribution II the unsteady wall shear variation is not much different from the one described in Fig. 1. In Fig. 2 we show now the same functions for the flow distribution III. Note again that as the flow relaxes to a steady in the mean, the unsteady wall shear leads again the quasi-steady by 45°. Yet, the mean of the quasi-steady variation was found by examining larger time solutions, not shown in the figure, to be again larger than the mean of the unsteady variation, but the amplitude of the quasi-steady variation is now larger than the amplitude of the unsteady variation. Figure 3 shows a set of velocity profiles at the station $s \cong 0.999$, upstream of separation. A detail of this figure in the vicinity of the wall is shown in Fig. 4 and both are in qualitative agreement with the experimental data of Ref. 14. Note that at this

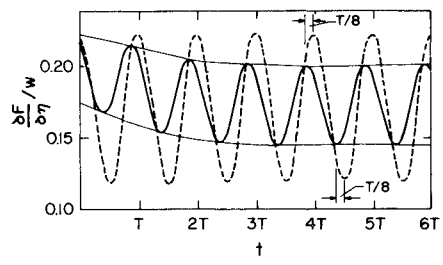

Fig. 2 Wall shear at $s \cong 0.999$ for $\omega = 3.16$, $b_1 = 0.1$, $C = 0.1$, and flow III; ------, quasi-steady; ————, unsteady.

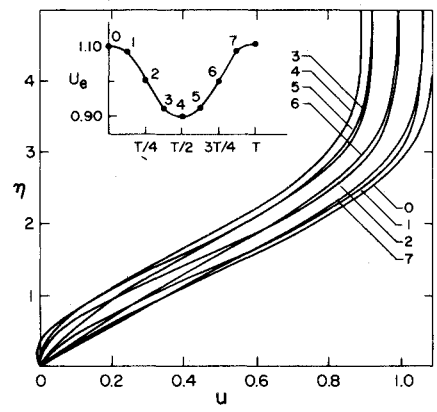

Fig. 3 Velocity profiles for one period, for flow I, at $s = 0.999$, $\omega = 3.16$, $b_1 = 0.1$, $C = 0.1$.

station, the wall shear oscillates between a negative and a positive extreme without any evidence of calculation breakdown, or singular behavior of the boundary-layer equations.

In Fig. 5 we have plotted the profile of the ratio $\Delta u/\Delta U_e$, the velocity amplitude over the outer flow amplitude, at the station $s = 0.999$, and against the distance from the wall measured in terms of the quantity $N(\omega/2)^{1/2}$, in order to compare with the theory of Lighthill and the experiments of Hill. This corresponds to the last downstream station that Hill took experimental data. Moreover Lighthill's application is based on the Kármán-Polhausen method which is known to be inaccurate in the neighborhood of separation. Our profile, an exact solution of the unsteady boundary-layer equation, shows an improvement over Lighthill's approximate method, which is based on the assumption of a very large frequency ω. It should be noted here that Hill's experimental device with an oscillating valve, imposes a disturbance to the oncoming stream and should therefore correspond to an oscillatory outer flow of the type I as Lighthill has indicated. Hill does not provide any data of the pressure distribution but instead includes in his report an analysis that corresponds to an outer flow distribution of the type II. For this reason in Fig. 6 we have plotted the same experimental data as well as Hill's improved analytical prediction. The experimental predictions of Hill, in Figs. 5 and 6, seem to have maxima closer to the wall compared to the present numerical results. We believe that this is because the experiments were performed in a closed channel. Stuart has indicated that the interference of the walls of a channel on the streaming phenomenon is negligible if the

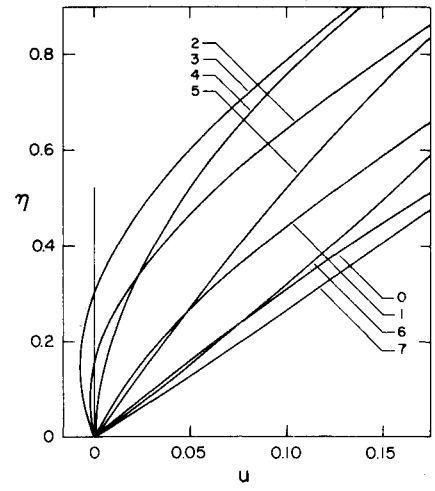

Fig. 4 Detail of velocity profile of Fig. 3.

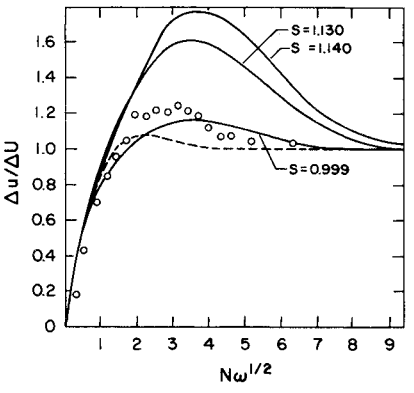

Fig. 5 Dimensionless amplitude of velocity oscillation for flow I, $\omega = 3.16$, $b_1 = 0.1$, $C = 0.1$; ———, present numerical results; ------, Lighthill[1] for $s = 1.000$, $\omega \gg 1$; ○, Hill for $s = 1.00$, experimental.

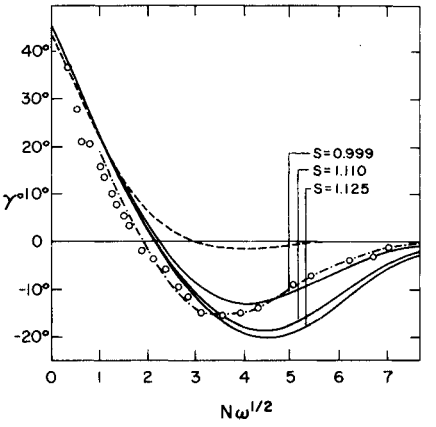

Fig. 7 Phase angle for flow I, $\omega = 2.9$, $b_1 = 0.1$, $C = 0.1$; ———, present numerical results; ------, Lighthill[1] for $s = 1.00$, $\omega \gg 1$: ·-·-·, Hill for s = theoretical; ○, Hill, experimental.

parameter $(d/D)^2 \cdot (\omega^* \nu / U_R{}^{*2})$ where d is the size of the model and D the width of the channel, is small. In Hill's case, if one takes L^* for d and the distance between the wall and the central pipe for D, then this parameter is larger than 0.4. The interference effect tends to confine the secondary streaming flow closer to the wall and hence gives rise to a maximum of $\Delta u/\Delta U_e$ at a distance $N(\omega/2)^{1/2}$ smaller than what the boundary-layer theory would predict.

In Fig. 7 the phase angle γ_0 between oscillations in the boundary layer and the outer flow is plotted again, against $N(\omega/2)^{1/2}$ for the outer flow I. All data indicate accurately that as $N \to 0$, the Stokes layer value $\gamma = 45°$, is approached. Note that away from the wall the phase angle changes sign and the boundary-layer flow anticipates the oscillation of the outer flow.

Figure 8 shows the profile of the steady streaming velocity u_s. This was derived by subtracting the mean of the unsteady velocity profile from the steady profile that was derived using the mean of the outer flow distribution. Note that the ratio of the coordinate N of the maximum u_s to the distance of this point from the edge of the boundary layer, is approximately equal to 0.30 at $s = 0.999$. Stuart predicted that for zero mean flow this ratio is equal to the parameter $\alpha = U_R{}^*/\omega^* L^*$. Note that $U_R{}^*$ in his case was the amplitude of oscillation, the only available velocity, whereas in our case it is the velocity defined in Sec. III. An estimate of α in our case gives $\alpha = 0.316$ which is in good agreement with the ratio of the two thicknesses as calculated here.

VI. Unsteady Separation

Let the extreme locations of the points of quasi-steady zero skin friction corresponding to $t = T/4$, $t = T/2$, and $t = 0$, where T is the period of oscillation, be denoted by S_1–S_3, respectively. The points S_2 and S_3 provide the limits of the excursions of the point of separation for quasi-steady flow. Let also the extreme upstream and downstream points of the unsteady excursions of the point of zero skin friction be, respectively, S_2' and S_3'. Note that according to the definition of Despard and Miller,[14] unsteady separation in oscillatory flow should occur at S_3'. Lighthill's oscillating flow with a Howarth mean distribution (flow distribution I) should provide a very interesting case whereby all points S_1–S_3 coincide, that is if the motion were quasi-steady, then the point of separation would remain unaffected by the oscillations of the outer flow. Figure 9 shows the temporal path of the point of zero skin friction for such a flow with S_1–S_3 all coinciding at $s = 1.222$. It is recalled that the initial solution at time $t = 0$ is a steady-state solution but the transient part corresponds to at most one or two periods and a flow steady in the mean is achieved. The points shown in this figure at the 3rd and 4th periods were calculated by the method of Lighthill[1] and the agreement seems to be satisfactory. It is seen in the figure that the minima of the excursions of the point of zero shear are in phase advance of 45° with respect to the outer flow.

Separation for the initial flow is marked by a zero skin friction as well as a Goldstein-type singularity.[19] We will make use here

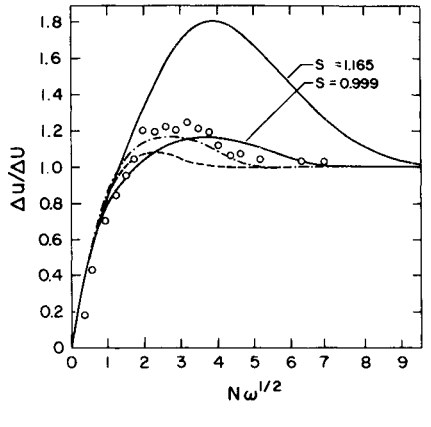

Fig. 6 Dimensionless amplitude of velocity oscillation for flow II, $\omega = 3.16$, $b_1 = 0.1$, $C = 0.1$; ———, present numerical results; ------, Lighthill[1] for $s = 1.00$, $\omega \gg 1$; ·-·-·, Hill for $s = 1.00$, theoretical; ○, Hill, experimental.

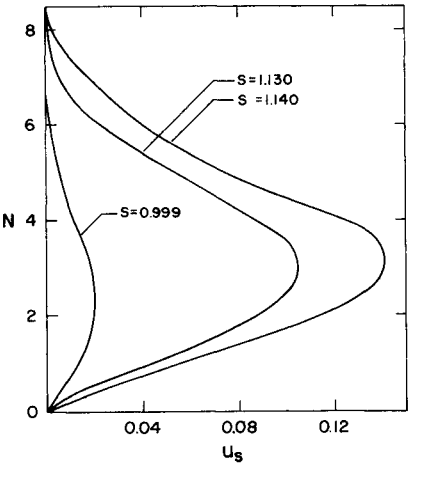

Fig. 8 Steady-streaming velocity profile for flow I, $\omega = 3.16$, $b_1 = 1.0$, $C = 0.1$.

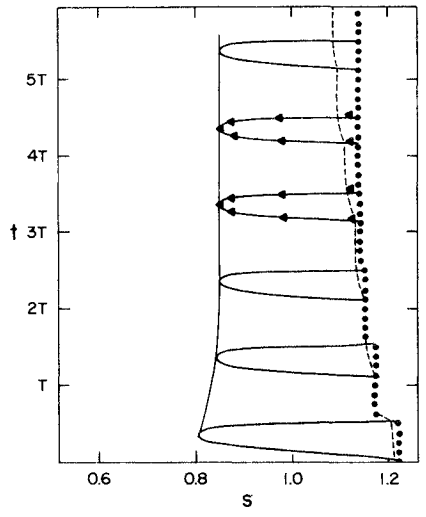

Fig. 9 Temporal paths of zero skin friction (————) and unsteady separation (•) for flow I, $\omega = 3.16$, $b_1 = 0.1$, $C = 0.1$; (------) distance $S_i(t_0)$ (see Sec. IV).

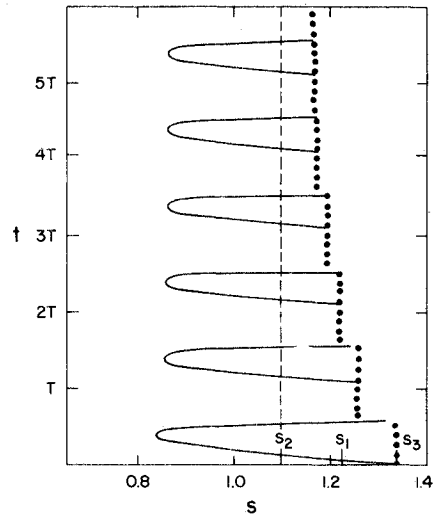

Fig. 11 Temporal paths of zero skin friction (————) and unsteady separation (•) for flow II, $\omega = 3.16$, $b_1 = 0.1$, $U_1 = 0.1$.

of the definition and criteria suggested by Sears and Telionis[17] (see also the review paper[15]). According to this definition the appearance of a singularity of the Goldstein type with its accompanying features, such as sharp steepening of properties like $\partial u/\partial s$, v, etc., and numerical evidence like increase of the number of iterations required for convergence and final inability to converge, should be used as a criterion for separation. It is recalled from Sec. II that the range of integration should collapse, that is, the point of separation should move upstream, at a rate at least equal to the speed of upstream propagation of disturbances, u_d. This condition is clearly in this case violated since the point of the separation singularity appears to be stationary at first at $s = 1.222$. In fact, we did not even observe the requirement of abandoning at least one mesh point in regions where the flow is reversed. This was achieved by using a Taylor extrapolation in order to store data at the final s-station. Mathematically one should integrate the functions u_d and u_p (see Sec. IV) with respect to time, plot them in Fig. 9 and discard any results to the right of any of them. We have shown in this figure schematically with a thin dashed curve, how this message should creep slowly upstream, eventually invalidating all the portion of the solution to the right of the upstream limit of the excursions of the point of zero shear.

There is still enough information to derive, though. We know that the point of separation does not move upstream, at least faster than u_d or u_p, which was often true in cases of transient flow.[20,21] Then we have indications that the numerical trick of a Taylor extrapolation may actually guide the solution to the correct final steady-in-the-mean flow. This is justified by the fact that our solution is in good agreement with Lighthill's analytical solution. On the other hand, the present calculations quickly attain periodicity all the way to the neighborhood of separation. It seems that the only hesitation would arise when attention is directed at the upstream propagation of the point of separation. Yet even in this case, after the transient part of the motion is left behind, periodicity is achieved and the singular behavior arrives at the station $s = 1.140$ and remains there. In Fig. 10 we have plotted the detail of the wall shear for one period in the neighborhood of separation, to show the familiar characteristic features of a Goldstein singularity.

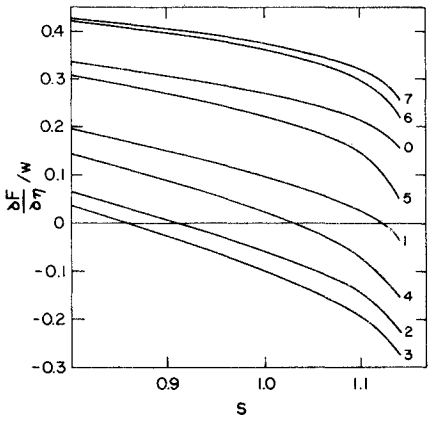

Fig. 10 The skin-friction variation at intervals within the 5th period as marked schematically in Fig. 3.

Some of the conclusions of Despard and Miller[14] are now verified numerically, but not all. A contradiction arises by considering the outer flow distribution chosen here, without even looking at the numerical results. The point of separation for oscillatory flows, as defined by Despard and Miller, is the point S_3'; that is, the furthest downstream point of the unsteady excursions of the point of zero skin friction. In this case (flow I) the quasi-steady separation, S_1, is located at $s = 1.222$, and Lighthill's analytical solution shows that S_3' is displaced towards the downstream direction of the point of quasi-steady separation S_1. Yet, Despard and Miller have found experimentally that the point of separation is always displaced upstream from its steady-state position. In the flow under consideration the numerical results indicate that this is indeed true and predict separation at $s = 1.140$. We may note, nevertheless, as the reviewer has suggested, that if we consider the extrapolation of the curves 5–7 of Fig. 10, then we may accept that the wall shear always vanishes at some point $s < 1.140$. With this interpretation the Despard and Miller findings are indeed satisfied.

Let us consider now the flow distribution II which probably resembles more closely the experimental pressure distribution that Despard and Miller have worked with. Now quasi-steady separation is at S_1 but our unsteady calculations start with a steady-state flow with separation at S_3. The results show (Fig. 11) that the separation singularity is displaced quickly upstream and arrives at a final station, $s = 1.160$, upstream of the points S_1 and S_3 but downstream of the point S_2.

Figure 12 shows the results for the outer flow distribution III. We observe again a region of hesitation where the Taylor extrapolation permits the integration to arrive at $s = 1.356$ at each time step. After the first period, though, the point of separation singularity starts propagating upstream and overcomes both the curves $\int u_d\,dt$ and $\int u_p\,dt$ (not shown in the figure).

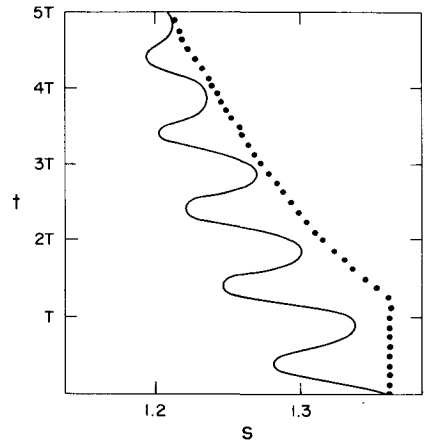

Fig. 12 Temporal path of zero skin friction (————) and unsteady separation (.) for flow III, $\omega = 3.16$, $b_1 = 0.1$, $C = 0.1$.

Now the point of separation appears to be very close to the point S_3', at least during the transient period, and hence our numerical results seem to be in agreement with the Despard and Miller definition. Figure 13 shows the skin-friction distribution for the third period of the oscillation which is well within the transient part of the motion. For later times the amplitude of the oscillations of the point of zero skin friction shows a tendency to decrease even more. This tendency was not evident at $s = 0.999$ upstream of this neighborhood where the amplitude of the wall shear was found to achieve periodicity, as shown in Fig. 2. This phenomenon perhaps requires further study.

The present data are the first available detailed information in the close vicinity of unsteady separation. Let us return to Fig. 5 where the velocity amplitude is plotted for two stations downstream of $s \cong 1.00$ for which information is available from Ref. 12, and hence much closer to separation. Note that the amplitude overshoot becomes much more pronounced in agreement with Despard and Miller. Figure 6 shows a similar tendency. In Fig. 7 we have plotted the phase angle function for two stations closer to separation. One would expect that this function would tend more towards its shear wave value but this does not seem to be the case.

In Fig. 8 it is shown that the streaming velocity grows considerably as separation is approached. In fact it appears that this quantity behaves singularly in the neighborhood of separation, that is it blows up with a square root of the distance from separation. This fact also requires more analytical and experimental investigation. One final remark appears pertinent here. It is possible that during the transient part of the motion separation moves momentarily downstream in each period of oscillation. This refinement of its motion cannot be picked up by the present method. This is perhaps why the paths of separation for some transient cases appear to consist of segments with apparent discontinuities at each period.

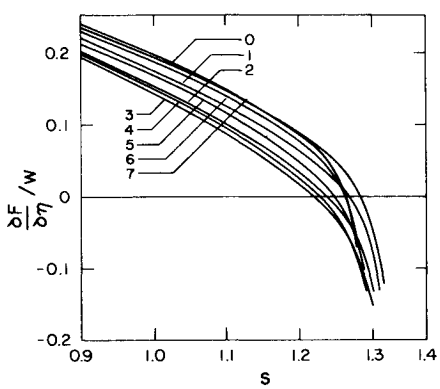

Fig. 13 The skin-friction variation at intervals within the 3rd period corresponding to Fig. 12 as marked schematically in Fig. 3.

VII. Conclusions and Comments

Numerical techniques were employed to investigate the basic features of unsteady boundary layers and separation. It was found that the mean of the steady oscillations deviates from the steady flow that corresponds to the mean of the outer flow distribution, which is in agreement with the findings of Schneck and Ostrach. The definition of steady or nonlinear streaming was extended to include the above phenomenon which is believed to have an important effect on the phenomenon of separation. Velocity profiles of streaming were calculated and it was found that this phenomenon corresponds, at least for cases of adverse pressure gradients, to a secondary flow directed in the upstream direction. The results were checked against previous theoretical and experimental data for regions well upstream of separation. The neighborhood of separation was investigated for the first time numerically. It was found that for the range of frequencies examined: 1) the point of separation stabilizes to a fixed location and remains insensitive to the oscillations of the outer flow; 2) the location of unsteady separation in oscillatory flows is always displaced upstream of the location of steady separation corresponding to the mean of the outer flow; and 3) the streaming velocity profile increases sharply as the neighborhood of separation is approached. Items 1) and 2) above were in qualitative agreement with the findings of Despard and Miller. Their criterion was found to be in agreement with the Sears and Telionis criterion in some of the cases considered. Comparative tests were provided on the relative merits of the two criteria.

References

[1] Lighthill, M. J., "The Response of Laminar Skin Friction and Heat Transfer to Fluctuations in the Stream Velocity," *Proceedings of the Royal Society of London*, Ser. A, Vol. 224, June 1954, pp. 1–23.

[2] Rott, N., "Unsteady Viscous Flow in the Vicinity of a Stagnation Point," *Quarterly Journal of Applied Mathematics*, Vol. 13, Jan. 1956, pp. 444–451.

[3] Glauert, M. B., "The Laminar Boundary Layer on Oscillating Plates and Cylinders," *Journal of Fluid Mechanics*, Vol. 1, May 1956, pp. 97–110.

[4] Rott, N. and Rosenzweig, M. L., "On the Response of the Laminar Boundary Layer to Small Fluctuations of the Free-Stream Velocity," *Journal of Aeronautical Sciences*, Vol. 27, Oct. 1960, pp. 741–747.

[5] Lam, S. H. and Rott, N., "Theory of Linearized Time-Dependent Boundary Layers," GSAE Rept. AFOSR TN-60-1100, Cornell University, Ithaca, N.Y., 1960.

[6] Ackerberg, R. C. and Phillips, J. H., "The Unsteady Laminar Boundary Layer on a Semi-Infinite Plate Due to Small Fluctuations in the Magnitude of the Free-Stream Velocity," *Journal of Fluid Mechanics*, Vol. 51, Pt. 1, Jan. 1972, pp. 137–157.

[7] Lin, C. C., "Motion in the Boundary Layer with a Rapidly Oscillating External Flow," *Proceedings of the Ninth International Congress of Applied Mechanics*, Brussels, Vol. 4, 1956, pp. 155–167.

[8] Gibson, W. E., "Unsteady Boundary Layers," Ph.D. thesis, 1957, MIT, Cambridge, Mass.

[9] Hall, M. G., "A Numerical Method for Calculating Unsteady Two-Dimensional Laminar Boundary Layers," *Ingenieur Archiv*, Vol. 38, 1969, pp. 97–106.

[10] Phillips, J. H. and Ackerberg, R. C., "A Numerical Method for Integrating the Unsteady Boundary-Layer Equations when there are Regions of Backflow," *Journal of Fluid Mechanics*, Vol. 58, Pt. 3, May 1973, pp. 561–579.

[11] Telionis, D. P., Tsahalis, D. Th., and Werle, M. J., "Numerical Investigation of Unsteady Boundary-Layer Separation," *The Physics of Fluids*, Vol. 16, No. 8, July 1973, pp. 968–973.

[12] Hill, P. G., "Laminar Boundary Layers in Oscillatory Flow," Sc.D. thesis, 1958, MIT, Cambridge, Mass.

[13] Hori, E., "Experiments on the Boundary Layer of an Oscillating Circular Cylinder," *Bulletin of the Japan Society of Mechanical Engineers*, Vol. 6, 1963, pp. 201–209.

[14] Despard, R. A. and Miller, J. A., "Separation in Oscillating Boundary-Layer Flows," *Journal of Fluid Mechanics*, Vol. 47, Pt. 1, May 1971, pp. 21–51.

[15] Sears, W. R. and Telionis, D. P., "Boundary Layer Separation in Unsteady Flow," presented at *Modern Developments of Fluid Mechanics*; a symposium in honor of the 70th birthday of S. Goldstein, Dec. 1973, also to appear in the *SIAM Journal of Applied Mathematics*.

[16] Moore, F. K., "On the Separation of the Unsteady Laminar Boundary Layer," in *Boundary Layer Research, Proceedings of a Symposium of the International Union of Theoretical and Applied Mechanics*, edited by H. Görtler, Freiburg, Germany, 1957, pp. 296–311.

[17] Sears, W. R. and Telionis, D. P., "Unsteady Boundary Layer Separation," in *Recent Research on Unsteady Boundary Layers, Proceedings of a Symposium of the International Union of Theoretical and Applied Mechanics*, Vol. I, edited by E. A. Eichelbrenner, Quebec, May 1971, pp. 404–447.

[18] Schenck, D. J. and Ostrach, S., "Pulsatile Blood Flow in a Diverging Circular Channel," TR FTAS/TR-73-86, 1973, Case Western Reserve Univ., Cleveland, Ohio.

[19] Brown, S. N. and Stewartson, K., "Laminar Separation," in *Annual Review of Fluid Mechanics*, edited by W. R. Sears, Vol. 1, 1969, Annual Reviews, Inc., Palo Alto, Calif., pp. 45–72.

[20] Telionis, D. P. and Tsahalis, D. Th., "The Response Separation to Impulsive Changes of Outer Flow," *AIAA Journal*, Vol. 12, No. 5, May 1974, pp. 614–619.

[21] Telionis, D. P. and Tsahalis, D. Th., "Unsteady Laminar Separation over Cylinders Started Impulsively from Rest," presented at the *24th International Astronautical Congress*, Baku, U.S.S.R., Oct. 1973; also to appear in *Acta Astronautica*.

[22] Stuart, J. T., "Double Boundary Layers in Oscillatory Viscous Flow," *Journal of Fluid Mechanics*, Vol. 24, Pt. 4, April 1966, pp. 673–687.

[23] Stuart, J. T., "Unsteady Boundary Layers," *Recent Research on Unsteady Boundary Layers, Proceedings of a Symposium of the International Union of Theoretical and Applied Mechanics*, edited by E. A. Eichelbrenner, Quebec, May 1971, Vol. 1, pp. 1–59.

[24] Werle, M. J. and Davis, R. T., "Incompressible Laminar Boundary Layers on a Parabola at an Angle of Attack: A Study of the Separation Point," *Journal of Applied Mechanics*, Vol. 39, No. 1, March 1973, pp. 7–12.

NOVEMBER 1974 AIAA JOURNAL VOL. 12, NO. 11

Radiation from an Array of Gray Circular Fins of Trapezoidal Profile

N. M. SCHNURR*
Vanderbilt University, Nashville, Tenn.
AND
C. A. COTHRAN†
NASA Marshall Space Flight Center, Huntsville, Ala.

A numerical method is developed to calculate the temperature distribution and radiation heat transfer for an annular fin and tube radiator, with fins having trapezoidal profiles. All surfaces are assumed gray and to emit and reflect diffusely. Radiative interactions between adjacent fins and between the fins and tube are included. The thermal conductivity of the fin material may vary linearly with temperature. The independent dimensionless parameters and their ranges are $\varepsilon = 0.8$–1.0, $r_i/r_o = 0.20$–0.67, $L/r_o = 0.25$–2.0, and $N_C = 0$–0.8. Results of a parametric study of the special case of circular fins of triangular profile having constant thermal conductivity are presented, and used to optimize a fin array with respect to minimum weight.

Nomenclature

B_i = radiosity of surface i
F = angle factor
k = thermal conductivity
k_0 = thermal conductivity at T_0
L = center to center spacing between fins
N = number of node points
q_r = radiant heat flux
Q = heat transfer from the fin array
Q_k = conduction heat transfer
Q_R = radiant heat transfer
r = radial distance
r_i = tube radius
r_o = fin outside radius
t = local fin thickness
t_i = thickness of fin at $r = r_i$
t_o = thickness of fin at $r = r_o$
T = temperature
T_0 = base temperature
ε = emissivity
Λ = matrix defined by Eq. (9)
σ = Stefan-Boltzmann constant
χ = matrix defined by Eq. (6)
ψ = inverse of the χ matrix
Ω = vector defined by Eq. (7)
$C = k/k_0$
$C' = (T_0/k_0)(dk/dT)$
$N_C = 2\sigma\varepsilon T_0^3 r_i^2/k_0 t_i$, the conduction number
$N_L = L/r_o$
$N_R = r_i/r_o$
$N_t = t_o/t_i$
$Q^* = Q/(2\pi r_i L\sigma T_0^4)$
$X = r/r_o$
$Y = t/t_i$
$\theta = T/T_0$

Received January 23, 1974; revision received May 8, 1974.
Index category: Radiation and Radiative Heat Transfer.
* Associate Professor, Department of Mechanical Engineering.
† Aerospace Engineer.